Phosphorus Chemical Shift Anisotropies in Solid Triphenyl Phosphite and *mer,trans*-Bis(triphenyl phosphite)tricarbonyl(thiocarbonyl)chromium(0), $Cr(CO)_3(CS)[P(OPh)_3]_2$

Yining Huang, Haewon L. Uhm, Denis F. R. Gilson,* and Ian S. Butler*

Department of Chemistry, McGill University, 801 Sherbrooke Street West, Montreal, Quebec, Canada H3A 2K6

Received June 9, 1993[⊗]

The ^{31}P chemical shift anisotropies have been measured for solid triphenyl phosphite, $P(OPh)_3$ (at 128 K), and the complex with the tricarbonyl(thiocarbonyl)chromium(0) moiety, *mer,trans*-$Cr(CO)_3(CS)[P(OPh)_3]_2$ (at 298 K). The shift tensor is axially symmetric in the phosphite ligand, and the major change upon complexation occurs for the components of the shift tensor perpendicular to the bond direction. The crystal structure of the chromium complex has been determined by single-crystal X-ray diffraction at 293 K. The complex crystallizes in the centric $P2_1/n$ (No. 14) space group with cell constants (at 20 °C) a = 8.166(3) Å, b = 11.530(2) Å, c = 20.183(2) Å, β = 96.43(1)°, and Z = 2. The molecule is disordered on a crystallographically imposed inversion center so that the thiocarbonyl ligand is superimposed on the *trans* carbonyl ligand (50:50).

Introduction

The wide chemical shift range and large scalar couplings make the ^{31}P nucleus an ideal probe for the study of stereochemistry, bonding interactions, and molecular dynamics. The large variation has been related to the electronegativity of the substituents, the bond angles between them, the σ- and π-bonding character involved, and the oxidation state of phosphorus. When a phosphorus ligand is coordinated to a metal, ^{31}P chemical shifts are also influenced by such factors as the bonding interaction between the phosphorus and the metal, the nature and the oxidation state of the metal, the coordination number, the influence of the trans ligand, and the position of the phosphorus ligand within the coordination sphere.[1] Most of the theoretical and experimental work on phosphorus compounds, however, has involved studies of isotropic chemical shifts in solution, and only a few investigations have dealt fully with the tensorial nature of the chemical shift interactions. The anisotropy of the chemical shift is inherently more informative than are the isotropic values. For example, in some cases, a change in molecular structure may lead to a small change in the isotropic shift but a significant difference in the components of the shift tensor. Few theoretical calculations of ^{31}P shielding tensors have been reported, and these are restricted to simple, small, and metal-free systems. Furthermore, it is rather difficult to calculate accurately the ^{31}P chemical shielding parameters because large basis sets including d functions are essential for reliable molecular orbital calculations.[2] The first step to improve the understanding of chemical shielding interactions is to investigate the variation of the principal components of the shift tensor with changes in molecular structure. While the shift anisotropy parameters for tertiary phosphines[3] and their complexes with transition metals[4] have been described, measurements on triphenyl phosphite and its complexes do not appear to have been reported. Several factors complicate the determination of the shift anisotropies of nuclei bonded to transition metal atoms. In particular, many transition metal nuclei possess high spins and large quadrupole moments. Chromium, however, has only one isotope with spin, ^{53}Cr, spin $^3/_2$, with 9.5% abundance, and no reports of ^{31}P shift anisotropies for complexes of chromium have appeared. The ^{31}P shift tensors of the free and bonded triphenyl phosphite ligands are presented here, together with the crystal structure of a chromium–triphenyl phosphite complex, *mer,trans*-$Cr(CO)_3(CS)[P(OPh)_3]_2$.

Experimental Section

Triphenyl phosphite (97%) was obtained from Omega Chemical Co. Inc. and was purified by vacuum distillation (300 ° C/3 Torr). The starting reagent, $Cr(CO)_5(CS)$, was prepared and purified as described in the literature.[5]

The *mer,trans*-$Cr(CO)_3(CS)[P(OPh)_3]_2$ complex was synthesized by the following procedure. A toluene solution (15 mL) containing $Cr(CO)_5(CS)$ (0.266 g, 1.13 mmol) and $P(OPh)_3$ (0.35 mL, 1.34 mmol) was heated at 103 °C for 2 h. The mixture was allowed to cool, and the solvent was removed under reduced pressure (Buchi rotavapor). The resulting yellow oil was adsorbed onto a small amount of silica gel, which was then placed on top of a 33 × 1.7 cm silica gel chromatography column. Two fractions were separated on the column by using 1:2 CH_2Cl_2–hexanes as the eluent. The first fraction contained a mixture of *cis*- and *trans*-$Cr(CO)_4[P(OPh)_3]_2$ (0.393 g, 56% yield). These compounds were identified by the similarity of their IR [ν(CO) region] to those of the PPh_3 analogs[6] and their ^{31}P-NMR spectra. Data for *cis*-$Cr(CO)_4[P(OPh)_3]_2$ are as follows. IR (hexanes) (cm^{-1}): ν(CO) 2057 s, 2005 m, 1971 vs, 1945 vw; ν(CS) 1256 s. ^{13}C-NMR ($CDCl_3$) at −20 °C: 333.6 [1C, d, CS, $J(^{31}P-^{31}C)$ = 26.4 Hz], 219.5 (1C, s, CO), 215.5 [2C, d, CO, $J(^{31}P-^{31}C)$ = 20.3 Hz] 211.7 ppm [1C, d, CO, $J(^{31}P-^{31}C)$ = 18.0 Hz]. ^{31}P-NMR ($CDCl_3$): 166.9 ppm (*s*). Data for *trans*-$Cr(CO)_4[P(OPh)_3]_2$ are as follows. IR (hexanes) (cm^{-1}): ν(CO) 2057 m, 2005 m, 1976 vs, 1945 vw; ν(CS) 1256 s. ^{13}C-NMR ($CDCl_3$) at −20 °C: 336.3 (1C, s, CS), 214.8 ppm [4C, d, CO, $J(^{31}P-^{31}C)$ = 18.0 Hz]. ^{31}P-NMR ($CDCl_3$): 168.5 ppm (s). The second fraction, upon solvent removal under reduced pressure, afforded a yellow solid. Recrystallization from CH_2Cl_2–hexanes gave yellow crystals of *mer,trans*-$Cr(CO)_3(CS)[P(OPh)_3]_2$ (0.108 g, 20% yield; mp 116–116.5 °C). Anal. Calcd for $C_{40}H_{30}O_9SP_2Cr$: C, 60.00; H, 3.78. Found: C, 59.36; H, 3.73. IR (hexanes) (cm^{-1}): ν(CO) 2030 s, 1989 m, 1949 vs; ν(CS) 1249 s. ^{13}C-NMR ($CDCl_3$) at −20 °C: 334.2 [1C, t, CS, $J(^{31}P-^{31}C)$ = 27.8 Hz], 218.7 [2C, t, CO, $J(^{31}P-^{31}C)$ = 20.8 Hz], 213.6 ppm [1C, t, CO, $J(^{31}P-^{31}C)$ = 17.4 Hz]. ^{31}P-NMR ($CDCl_3$): 173.0 ppm (s).

The IR spectra were recorded on a Bomem MB-100 FT spectrometer equipped with a KBr beamsplitter and a standard TGS detector. The ^{13}C- and ^{31}P-NMR spectra were measured for concentrated solutions on a Varian XL-300 spectrometer. The solid-state ^{31}P-NMR measurements were performed on a Chemagnetics CMX-300 spectrometer operating

[⊗] Abstract published in *Advance ACS Abstracts,* January 15, 1994.

(1) Pregosin, P. S.; Kunz, R. W. ^{31}P and ^{13}C NMR of Transition Metal Phosphine Complexes. *NMR Basic Principles and Progress*, Vol. 16; Springer-Verlag: Berlin, 1979.
(2) Fleischer, U.; Schindler, M.; Kutzelnigg, W. *J. Chem. Phys.* **1989**, *86*, 6337.
(3) Penner, G. H.; Wasylishen, R. E. *Can. J. Chem.* **1989**, *67*, 1909.
(4) Linder, E.; Fawzi, R.; Mayer, H. A.; Eicheie, K.; Pohmer, K. *Inorg. Chem.* **1991**, *30*, 1102.
(5) English, A. M.; Plowman, K. R.; Baibich, I. M.; Hickey, J. P.; Butler, I. S. *J. Organomet. Chem.* **1981**, *205*, 177.
(6) Dombek, B. D.; Angelici, R. J. *Inorg. Chem.* **1976**, *15*, 1089.

0020-1669/94/1333-0804$04.50/0

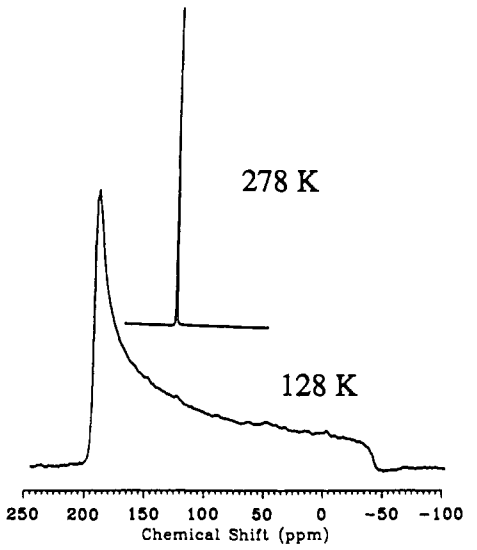

Figure 1. Static ^{31}P-NMR spectra of $P(OPh)_3$.

Table 1. ^{31}P-NMR Chemical Shift Anisotropies[a,b]

compd	δ_{11}	δ_{22}	δ_{33}	δ_{iso}	$\Delta\delta$
$P(OPh)_3$[c]	199	199	−41	119	−240
mer,trans-$Cr(CO)_3(CS)[P(OPh)_3]_2$[d]	315	286	−88	171	−389
	305	279	−83	167	−375

[a] Values of principal elements and isotropic shifts are in ppm, relative to external 85% H_3PO_4. [b] Uncertainties are ± 10 and ±18 ppm for the data obtained from the MAS and static spectra, respectively. [c] Data measured at 128 K. [d] Data measured at 298 K.

Table 2. Crystallographic Data for *mer,trans*-$Cr(CO)_3(CS)[P(OPh)_3]_2$

chem formula $C_{40}H_{30}CrO_9P_2S$	fw 800.68
lattice params	space group $P2_1/n$ (No. 14)
a = 8.166(3) Å	T = 20 °C
b = 11.530(2) Å	λ = 0.710 69 Å
c = 20.183(2) Å	ρ_{calcd} = 1.408 g cm^{-3}
β = 96.43(1)°	μ = 4.84 cm^{-1}
V = 1888.5 Å^3	$R(F_o)$ = 0.071[a]
Z = 2	$R_w(F_o)$ = 0.072[b]

[a] $R = \sum||F_o| - |F_c||/\sum|F_o|$. [b] $R_w = [(\sum\omega(|F_o| - |F_c|)^2)]^{1/2}$.

at 121.28 MHz, with cross-polarization (CP) and high-power proton decoupling. The 90° pulse width was about 2.5 μs. The CP-MAS spectra were recorded for samples packed into a bullet-type zirconia rotor (7.5-mm diameter). The tensor values of *mer,trans*-$Cr(CO)_3(CS)[P(OPh)_3]_2$ were determined only from the MAS spectra, by the Hertzfeld–Berger graphical method,[7] from spectra acquired at two different spinning rates. The tensor components for triphenyl phosphite were obtained from nonspinning spectra only by the phase-cycled Hahn echo pulse sequence (90°–τ–180°).[8] Measurements for the phosphite complex were made at room temperature, but the spectra of $P(OPh)_3$ were recorded at low temperature where the sample temperature was regulated to within ±2 K by a RKC REX-C1000 temperature controller.

X-ray diffraction measurements were conducted on a Rigaku AFC6S diffractometer with graphite-monochromated Mo Kα radiation. A yellow needle crystal with approximate dimensions 0.25 × 0.20 × 0.50 mm was mounted on a glass fiber. Cell constants and an orientation matrix for data collection were obtained from a least-squares refinement using the setting angles of 25 carefully centered reflections in the range 15.34 < 2θ < 24.63°. The data were collected at room temperature using the ω–2θ scan technique to a maximum 2θ value of 50° at a scan rate of 16°/min. Of the 3917 reflections which were collected, 3507 were unique. The intensities of three representative reflections were measured after every 150 reflections and remained constant throughout the data collection. An empirical absorption correction was applied, and the data were corrected for Lorentz and polarization effects. The structure was solved by direct methods.[9] The non-hydrogen atoms were refined anisotropically. The final cycle of the full-matrix least-squares refinement was based on 1505 observed reflections [$I > 3.00\sigma(I)$] and 241 variable parameters and converged with weighted and unweighted agreement factors of R =

(7) Herzfeld, J.; Berger, A. E. *J. Chem. Phys.* **1980**, *73*, 6021.
(8) Rance, M.; Byrd, R. A. *J. Magn. Reson.* **1983**, *52*. 221.

Table 3. Positional Parameters and B(eq) Values (Å^2) for $Cr(CO)_3(CS)(P(OPh)_3)_2$

atom	x	y	z	B(eq)
Cr	0	0	0	3.2(1)
S[a]	0.0476(7)	−0.2400(4)	−0.0775(2)	7.8(3)
P	0.0900(3)	0.0889(2)	−0.0893(1)	3.0(1)
O(1)	−0.0407(7)	0.0983(5)	−0.1548(3)	3.6(3)
O(2)	0.2370(7)	0.0186(5)	−0.1167(3)	3.8(3)
O(3)	0.1513(8)	0.2226(5)	−0.0887(3)	3.9(3)
O(4)	0.3511(9)	−0.0206(7)	0.0695(4)	6.1(4)
O(5)[a]	0.0476	−0.2400	−0.0775	7.8
C(1)	−0.203(1)	0.271(1)	−0.1595(5)	4.8(5)
C(2)	−0.272(1)	0.366(1)	−0.1961(7)	6.6(7)
C(3)	−0.240(2)	0.379(1)	−0.2626(7)	7.4(8)
C(4)	−0.143(2)	0.301(1)	−0.2884(6)	7.2(8)
C(5)	−0.073(1)	0.211(1)	−0.2537(4)	4.4(5)
C(6)	−0.106(1)	0.1961(8)	−0.1891(4)	3.3(4)
C(7)	0.384(1)	0.1160(9)	−0.1968(4)	4.0(5)
C(8)	0.431(1)	0.120(1)	−0.2613(5)	4.8(6)
C(9)	0.375(2)	0.039(1)	−0.3076(5)	5.5(6)
C(10)	0.275(2)	−0.048(1)	−0.2917(5)	5.9(7)
C(11)	0.225(1)	−0.054(1)	−0.2280(6)	5.4(6)
C(12)	0.282(1)	0.0276(9)	−0.1829(4)	3.4(4)
C(13)	0.393(1)	0.230(1)	−0.0098(5)	5.5(6)
C(14)	0.489(2)	0.292(1)	0.0409(7)	7.6(8)
C(15)	0.433(2)	0.397(2)	0.0599(7)	8(1)
C(16)	0.292(2)	0.444(1)	0.0334(7)	8(1)
C(17)	0.197(1)	0.383(1)	−0.0170(5)	5.7(6)
C(18)	0.249(1)	0.278(1)	−0.0371(4)	4.1(5)
C(19)	0.025(1)	−0.140(1)	−0.0445(5)	4.7(5)
C(20)	0.217(1)	−0.0127(9)	0.0416(4)	4.0(5)
H(1)	−0.2238	0.2594	−0.1147	5.8
H(2)	−0.3382	0.4205	−0.1763	7.9
H(3)	−0.2863	0.4411	−0.2889	8.9
H(4)	−0.1231	0.3105	−0.3336	8.6
H(5)	−0.0021	0.1596	−0.2735	5.3
H(6)	0.4217	0.1721	−0.1641	4.8
H(7)	0.5028	0.1801	−0.2731	5.8
H(8)	0.4061	0.0435	−0.3515	6.5
H(9)	0.2386	−0.1050	−0.3240	7.1
H(10)	0.1533	−0.1132	−0.2166	6.5
H(11)	0.4272	0.1562	−0.0243	6.5
H(12)	0.5906	0.2616	0.0613	9.1
H(13)	0.4987	0.4385	0.0937	9.9
H(14)	0.2560	0.5165	0.0486	10.1
H(15)	0.0969	0.4156	−0.0374	6.8

[a] One-half occupancy.

Table 4. Intramolecular Distances (Å) Involving Non-Hydrogen Atoms with Estimated Standard Deviations in the Least Significant Figure Given in Parentheses

Cr–P	2.267(2)	C(2)–C(3)	1.40(2)
Cr–P	2.267(2)	C(3)–C(4)	1.33(2)
Cr–C(19)	1.87(1)	C(4)–C(5)	1.34(1)
Cr–C(19)	1.87(1)	C(5)–C(6)	1.37(1)
Cr–C(20)	1.88(1)	C(7)–C(8)	1.40(1)
Cr–C(20)	1.88(1)	C(7)–C(12)	1.37(1)
S–C(19)	1.36(1)	C(8)–C(9)	1.37(1)
P–O(1)	1.607(6)	C(9)–C(10)	1.35(2)
P–O(2)	1.597(6)	C(10)–C(11)	1.39(1)
P–O(3)	1.621(6)	C(11)–C(12)	1.35(1)
O(1)–C(6)	1.40(1)	C(13)–C(14)	1.42(2)
O(2)–C(12)	1.43(1)	C(13)–C(18)	1.35(1)
O(3)–C(18)	1.39(1)	C(14)–C(15)	1.36(2)
O(4)–C(20)	1.17(1)	C(15)–C(16)	1.33(2)
O(5)–C(19)	1.36(1)	C(16)–C(17)	1.39(2)
C(1)–C(2)	1.40(1)	C(17)–C(18)	1.37(1)
C(1)–C(6)	1.36(1)		

(9) (a) Gilmore, C. J. *J. Appl. Crystallogr.* **1984**, *17*, 42. (b) Beirskens, P. T. Direct Methods for Difference Structures. Technical Report 1984/1, Crystallography Laboratory, Toernooiveld, 6525 Ed Nijmegen, The Netherlands.

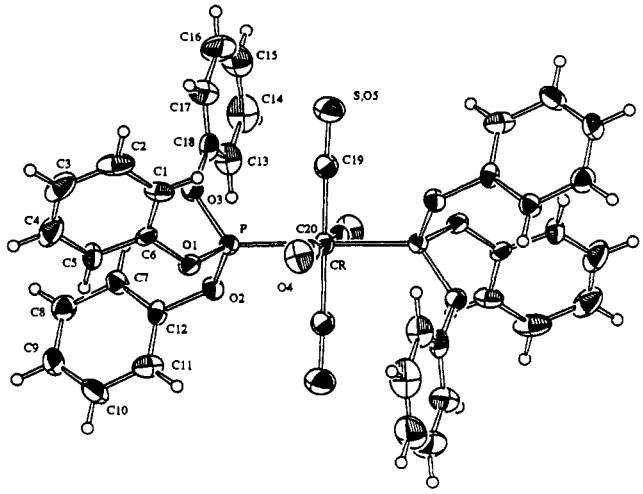

Figure 2. Molecular structure of *mer,trans*-$Cr(CO)_3(CS)[P(OPh)_3]_2$. ORTEP representations are at 30% probability.

Table 5. Intramolecular Bond Angles (deg) Involving Non-Hydrogen Atoms

P–Cr–P	180.00	C(1)–C(2)–C(3)	119(1)
P–Cr–C(19)	86.8(3)	C(2)–C(3)–C(4)	119(1)
P–Cr–C(19)	93.2(3)	C(3)–C(4)–C(5)	123(1)
P–Cr–C(20)	90.9(3)	C(4)–C(5)–C(6)	118(1)
P–Cr–C(20)	89.1(3)	O(1)–C(6)–C(1)	120.3(9)
P–Cr–C(19)	93.2(3)	O(1)–C(6)–C(5)	118.1(9)
P–Cr–C(19)	86.8(3)	C(1)–C(6)–C(5)	122(1)
P–Cr–C(20)	89.1(3)	C(8)–C(7)–C(12)	117.1(9)
P–Cr–C(20)	90.9(3)	C(7)–C(8)–C(9)	120(1)
C(19)–Cr–C(19)	180.00	C(8)–C(9)–C(10)	121(1)
C(19)–Cr–C(20)	89.8(4)	C(9)–C(10)–C(11)	120(1)
C(19)–Cr–C(20)	90.2(4)	C(10)–C(11)–C(12)	118(1)
C(19)–Cr–C(20)	90.2(4)	O(2)–C(12)–C(7)	118.2(9)
C(19)–Cr–C(20)	89.8(4)	O(2)–C(12)–C(11)	118.5(9)
C(20)–Cr–C(20)	180.00	C(7)–C(12)–C(11)	123.3(9)
Cr–P–O(1)	116.1(2)	C(14)–C(13)–C(18)	118(1)
Cr–P–O(2)	111.7(2)	C(13)–C(14)–C(15)	119(1)
Cr–P–O(3)	123.4(2)	C(14)–C(15)–C(16)	123(1)
O(1)–P–O(2)	101.9(3)	C(15)–C(16)–C(17)	118(1)
O(1)–P–O(3)	96.8(3)	C(16)–C(17)–C(18)	120(1)
O(2)–P–O(3)	104.0(3)	O(3)–C(18)–C(13)	121(1)
P–O(1)–C(6)	130.0(6)	O(3)–C(18)–C(17)	117(1)
P–O(2)–C(12)	124.6(6)	C(13)–C(18)–C(17)	122(1)
P–O(3)–C(18)	126.2(6)	Cr–C(19)–S	178.4(8)
C(2)–C(1)–C(6)	119(1)	Cr–C(20)–O(4)	177.8(8)

0.071 and R_w = 0.072, respectively. All calculations were performed using the TEXSAN crystallographic software package.[10]

Results and Discussion

Triphenyl Phosphite. Triphenyl phosphite is a liquid at room temperature and freezes at 292 K. At room temperature, a sharp single line was observed in its ^{31}P-NMR spectrum (Figure 1), which, on cooling, persisted far below the melting point, and a typical CSA powder pattern was not observed until 153 K, indicating that the isotropic motion exists over a wide temperature range. It is not clear, at this stage, if the sample supercooled or formed a plastic phase in which the molecule still undergoes isotropic reorientation. Upon warming, the wide powder pattern was observed throughout the temperature range from 128 to 278 K, where the powder pattern spectrum transformed into a sharp singlet, suggesting that there might be a plastic phase existing between 278 K and the melting point. The tensor values and anisotropy for $P(OPh)_3$ are given in Table 1. The powder pattern of triphenyl phosphite in the rigid lattice is axially symmetric. The crystal structure of this compound is not known, but the observation of an axially symmetric powder pattern implies that the C_3 symmetry of this molecule is preserved in a rigid lattice or, at least, the deviation from C_3 symmetry, if any, is not large enough to remove the degeneracy of the δ_{11} and δ_{22} components. Axial symmetry of the shift tensor appears to be common in tertiary phosphines, for example, even though the C_3 symmetry is not present.[2] The isotropic chemical shift of the ^{31}P nucleus shifts from −5.6 ppm for PPh_3 to the much more deshielded +127 ppm value for $P(OPh)_3$. When the individual tensor values are not known, it is not clear if such a shift results from all the tensor components systematically shifting downfield or if only the change in one particular element is responsible for the observed difference. The δ_{33} component of the phosphite shift anisotropy is identical to that of the phosphine but the $\delta_\parallel$ component is much more deshielded than is the corresponding component in triphenylphosphine, and it is this component which is responsible for the differences in the isotropic chemical shift and the shielding anisotropy between these two compounds. The shielding anisotropy, defined as $\Delta\delta = \delta_{33} - (\delta_{11} + \delta_{22})/2$, is about five times larger than that of PPh_3.[3] The electronegativity of the substituents on phosphorus and the angles between them have been considered to be the two most important variables influencing the ^{31}P isotropic chemical shift. For $P(OPh)_3$, the smaller cone angle (128°), compared to that of PPh_3 (145°),[9] and large electronegativity of the oxygen atoms certainly account for the difference in isotropic chemical shift for the two compounds. The shielding tensor values indicate that these electronic and steric effects influence only the $\delta_\perp$ component, leaving $\delta_\parallel$ unaffected.

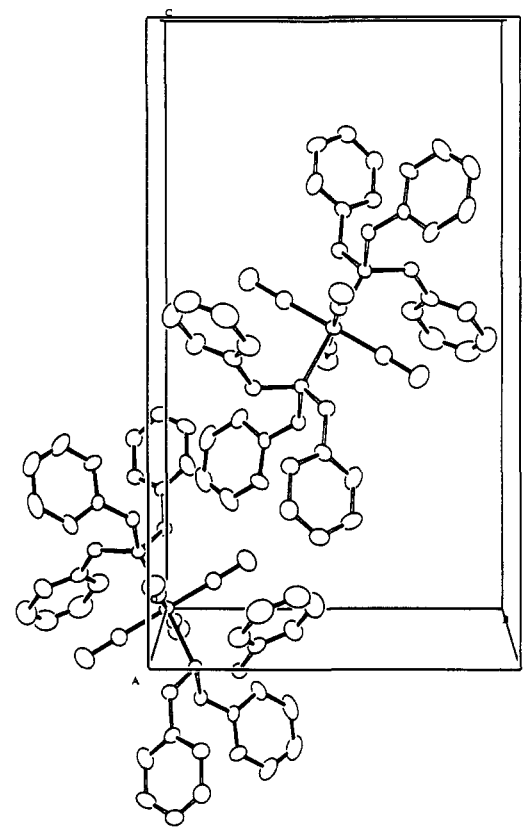

Figure 3. Crystal packing of *mer,trans*-$Cr(CO)_3(CS)[P(OPh)_3]_2$.

***mer,trans*-$Cr(CO)_3(CS)[P(OPh)_3]_2$.** Details of the crystal structure determination of this complex are given in Table 2. The final atomic positions and selected bond lengths and bond angles are listed in Tables 3–5, respectively. The molecule is located at a crystallographically imposed center of symmetry with disorder between the thiocarbonyl group and its *trans* carbonyl ligand (50:50). Thus, the sulfur and oxygen atoms cannot be distinguished and any differences in bond lengths are obscured. A

(10) TEXSAN-TEXRAY Structure Analysis Package, Molecular Structure Corp., 1985.
(11) Tolman, C. A. *Chem. Rev.* **1977**, *77*, 313.

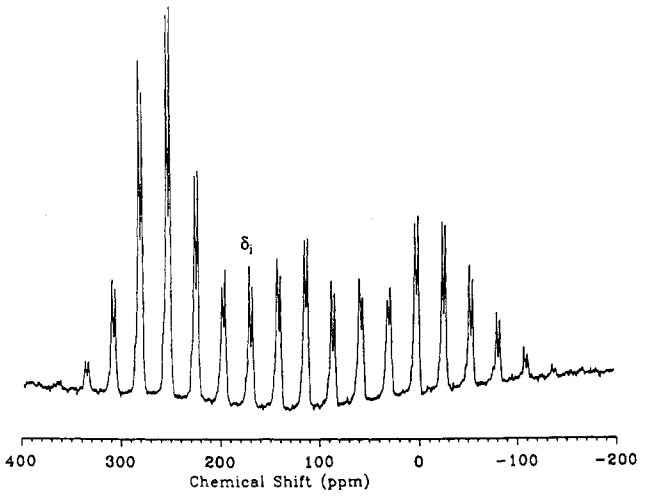

Figure 4. ^{31}P-CP-MAS spectra of *mer,trans*-$Cr(CO)_3(CS)[P(OPh)_3]_2$ at 298 K. The spinning rate is 3.4 kHz.

view of the molecule is shown in Figure 2, while the molecular packing is illustrated in Figure 3.

The values of the chemical shielding tensor components for *mer,trans*-$Cr(CO)_3(CS)[P(OPh)_3]_2$ are given in Table 1. Figure 4 shows a CP-MAS spectrum of this complex, and two phosphorus chemical shifts, due to crystallographic inequivalence, are clearly distinguishable. Upon complexation to chromium, the degeneracy of the parallel components is removed with the major changes, about 100 ppm, occurring for the perpendicular components. The O–P–O [101.9(3), 96.8(3), 104.0(3)°] and Cr–P–O [116.1(2), 111.7(2), 123.4(2)°] bond angles (Table 5) show that O(3) and the attached phenyl ring are clearly different and this phenyl ring is nearly perpendicular to the Cr–P bond direction (Figure 2). Although both the carbonyl and thiocarbonyl ligands are good π-acceptors, the CS ligand is better than CO.[12] A larger difference between the two perpendicular components would be anticipated but was not observed. The 382 ppm anisotropy is quite large. Triphenyl phosphite is considered to be a strong π-acceptor ligand, and the π-bonding interaction between the metal and the phosphorus atoms should be even stronger when there are two $P(OPh)_3$ ligands *trans* to each other. For instance, the average Cr–P bond length in *trans*-$Cr(CO)_4[P(OPh)_3]_2$ of 2.252 Å[13] is significantly shorter than that in $Cr(CO)_5[P(OPh)_3]$, 2.309 Å.[14] Also, the average Cr–P bond distance in *trans*-$Cr(CO)_3(CS)[P(OPh)_3]_2$ of 2.267 Å suggests the presence of strong π-bonding interactions. Therefore, the change in the parallel component upon complexation reflects the redistribution of electron density in the planes containing the δ_{33} axis due to the bonding between the Cr and P atoms. The upfield shift for the parallel component indicates that the paramagnetic contribution to this component decreases upon coordination to the metal. The paramagnetic components of the shift tensor are sensitive to changes in electronic density in the plane perpendicular to the tensorial direction. Since the δ_{33} component is directed along the Cr–P bond, differences in the metal–phosphorus bonding should be reflected in changes in the values of δ_{11} and δ_{22}.

The concept of a "coordination chemical shift", the isotropic shift of a complex minus the isotropic shift of the free ligand, has been widely used in phosphorus coordination chemistry, in particular for transition metal–phosphine complexes.[1,3] The present study has demonstrated that a comparison of the individual tensor components for different complexes is more informative than the use of averaged isotropic values in attempting to understand the nature of metal–ligand bonding.

Acknowledgment. This research was supported by grants to D.F.R.G. and I.S.B. from the NSERC (Canada) and FCAR (Québec). Y.H. acknowledges the award of a Graduate Fellowship from McGill University. Dr. J. Britten is thanked for his assistance in the X-ray diffraction study.

Supplementary Material Available: A complete X-ray structure report including tables of crystal data, text containing details of the structure determination, and tables of atom coordinates, bond lengths, bond angles, anisotropic thermal parameters, and hydrogen atom locations (18 pages). Ordering information is given on any current masthead page.

(12) Butler, I. S. *Acc. Chem. Res.* **1977**, *10*, 359.

(13) Preston, H. S.; Stewart, J. M.; Plastas, H. J.; Grim, S. O. *Inorg. Chem.* **1972**, *11*, 161.

(14) Plastas, H. J.; Stewart, J. M.; Grim, S. O. *Inorg. Chem.* **1973**, *12*, 265.